Journal of Materials Chemistry

Cite this: *J. Mater. Chem.*, 2011, **21**, 12717

www.rsc.org/materials

PAPER

Design and synthesis of photoactive ionic amorphous molecular materials†

Alexi K. Nedeltchev, Haesook Han and Pradip K. Bhowmik*

Received 20th April 2011, Accepted 1st July 2011
DOI: 10.1039/c1jm11735a

Compounds bearing electrostatic charges have unique properties including outstanding ionic-conductivity when compared with neutral ones. On the other hand, amorphous molecular materials harness the advantages of small molecules with high purity, defined structures and monodispersity, while still being easily processable into thin films and fibers. Here, we report a series of bis(pyridinium salt)s that combine these properties to form ionic amorphous molecular materials. Their design allowed them to vitrify efficiently upon slow cooling. They exhibited glass-transition temperatures in the range of 81–191 °C and had excellent thermal stabilities of up to 461 °C. Fibers were easily drawn from their melts that were visible to the naked eye. Although they were completely conjugated and had large molecular sizes, they were soluble in many common organic solvents. Additionally, they fluoresced blue and green light in both solution and solid states. They could be useful for high-performance applications in opto- and microelectronic fields, among others.

Introduction

Amorphous molecular materials are atypical due to their thermodynamic non-equilibrium state; as a result, they exhibit glass-transition (T_g) temperatures.[1–3] They have gained a significant interest in the scientific community since they can form stable thin films as similar to amorphous polymeric materials. Molecular glasses possess several advantages over polymers since they can be prepared in high purity, have defined molecular structures without end groups and are monodispersed. Similarly, they outperform small crystalline molecules because they are homogeneous without grain boundaries, transparent, and do not scatter light.[1–7] This suite of properties makes amorphous molecular materials attractive for applications in opto- and microelectronics including organic light emitting diodes (OLEDs), light emitting electrochemical cells (LECs), organic field effect transistors (OFETs), organic photovoltaic cells and organic lasers, among others.[8–12] To prepare molecular compounds that vitrify efficiently is a challenging task since small compounds tend to crystallize readily. In his several reviews, Shirota identified a few important structural characteristics that were found to promote a glassy state in these molecular materials. Large molecular size, rigidity, asymmetricity and presence of bulky substituents are the general guidelines that need to be met to make amorphous molecular materials.[4,5]

In parallel efforts, numerous organic ionic compounds have been developed as ionic liquids, both protic and aprotic. Due to their unique solvating properties, low vapor pressure and low toxicity, they are useful for versatile applications that range from reaction media for organic and polymer synthesis to extractors to lubricants.[13–17] Most recently, they have been investigated as potential drugs since they lack the phenomenon of polymorphism.[18] Even though there is an abundance of these organic salts, up until now they have not been seriously considered as amorphous molecular materials because most of them are either highly crystalline or ionic liquids. They are usually studied as materials in either crystalline or liquid states.[19] Moreover, they have low thermal transitions and only moderate thermal stabilities.

Here we demonstrate a series of bis(pyridinium salt)s that combine amorphous character with electrostatic charges to form high-performance ionic amorphous molecular materials. They have excellent thermal stabilities that are as high as 461 °C, which are comparable with those of high-performance polymers. They exhibit high T_g temperatures that are desirable for most applications and can be effectively tuned by modifications of either the dications or the anions. Since they have good solubilities in a wide range of common organic solvents, they can be processed efficiently into thin films and fibers from their melts and/or solutions. Additionally, they emit blue or green light in both the solution and solid states. We believe that this series of materials is the cornerstone that would open up a new field in materials science. Their general chemical structures and designations are shown in Scheme 1.

Results and discussions

Thermal transitions

The thermal transitions of the materials described herein, compiled in Table 1, were found to be strongly dependent on the

Department of Chemistry, University of Nevada Las Vegas, 4505 Maryland Parkway Box 454003, Las Vegas, NV, 89154, USA. E-mail: pradip.bhowmik@unlv.edu

† Electronic supplementary information (ESI) available. See DOI: 10.1039/c1jm11735a

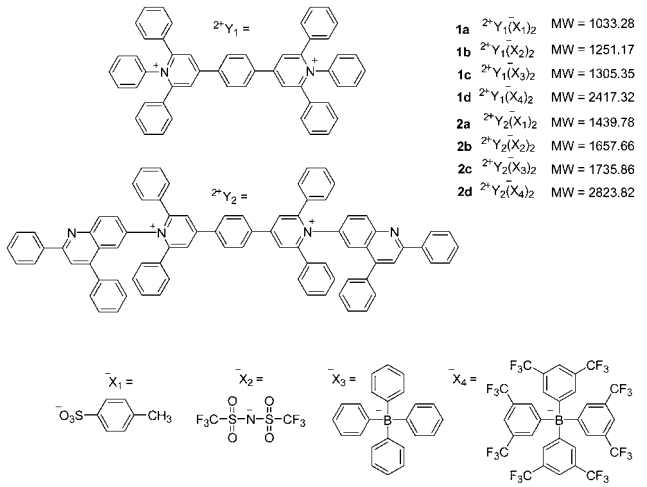

Scheme 1 Chemical structures of bis(pyridinium salt)s **1a–d** and **2a–d**.

nature of the anions as well as of the side groups appended to the dications. This variation of the T_g values by the exchange of the anions is commonly manifested in many poly(pyridinium salt)s and viologen polymers.[20–22] Fig. 1a shows the thermal transitions for the first set of ionic molecular materials (**1a–d**). Compound **1a**, which is composed of Y_1 and X_1, showed a stable glass transition T_g at 151 °C upon slow cooling at a rate of 10 °C min^{-1} after melting the solvent induced crystals. Interestingly, exchanging the anion from tosylate (X_1) to triflimide (X_2) strongly promoted the rate of crystallization in compound **1b**, which crystallized readily after cooling from its melt. A glassy state of **1b** was obtained by rapidly cooling a melted sample with liquid nitrogen, which had a T_g of 115 °C. This approach was undesirable since, by doing so, cracks and deformations formed in the glassy states. From this point onward, we undertook two approaches to improve the glass-forming property. The first one was to make materials with two additional anions. In the second approach, we prepared a dication with bulky asymmetric quinoline groups (Y_2). Tetraphenylborate (X_3) and tetrakis[3,5-bis (trifluoromethyl)phenyl]borate (X_4) were used as anions, but with limited success. Y_1 paired with X_3 afforded a crystalline compound **1c** that did not melt before its decomposition temperature; while Y_1 paired with X_4 (compound **1d**) did melt and did form glass with T_g at 81 °C. The second set of materials used dication Y_2, which had asymmetric kinked quinoline moieties that promoted the amorphous state and increased the T_g temperatures of the materials (Fig. 1b). Compound **2a** (Y_2 paired with X_1) produced a material that vitrified at 190 °C after melting. This chemical structure results in an increase in 39 °C of the T_g compared to **1a**, which had the same anion. After melting the solvent induced crystals, compound **2b** sustained a stable glassy state upon slow cooling at a rate of 10 °C min^{-1}, unlike compound **1b**, which crystallized readily. Its T_g was also substantially increased by 54 °C compared to **1b**. The last two bulky anions afforded amorphous materials that could not be crystallized by means of a solvent. Compound **2c** had a T_g at 185 °C in the first heating cycle and 191 °C in the second heating cycle. Compound **2d** had a T_g at 119 °C in the second heating cycle, which is 38 °C higher compared with that of compound **1d**. From these data we can deduce that the thermal transitions and glass-forming properties are governed by the chemical architectures of the dications and the anions. In the first set of materials, only compound **1a** and **1d** vitrified efficiently, whereas compound **1b** could be formed into glass only by rapid cooling and compound **1c** did not melt at all. In the second set of materials, large quinoline side groups were introduced where all the materials sustained stable amorphous states and their T_g temperatures were increased substantially. Here, we should stress that most of the materials formed a glassy state upon slow cooling—this method is essential in order to make uniform glasses with no cracks or deformations, which are beneficial to the fabrication for material devices.

Thermal stability

It is an important feature used for materials operating at harsh conditions. The materials in this study exhibited decomposition temperatures in the range of 257–461 °C, some of which are comparable to the thermal stabilities of high performance polymers such as Kevlar.[25] We established that chemical modification of either the dications or the anions has an effect on the thermal decomposition temperatures of ionic materials much like poly (pyridinium salt)s and viologen polymers.[19–21] The exchange of tosylate (X_1) to triflimide (X_2) resulted in an increase of the thermal stability in both sets of compounds by 79 °C in both cases (Fig. S1a†). X_2 (compared to X_1) had significantly weaker nucleophilic character. Therefore, it decomposed the dication nucleophilically at higher temperatures. Additionally, the exchange of tetraphenylborate (X_3) to tetrakis[3,5-bis

Table 1 Thermal properties of bis(pyridinium salt)s of **1a–d** and **2a–d**

Compound	1a	1b	1c	1d	2a	2b	2c	2d
1st heating	346 °C (T_m)	115 °C (T_g),[a] 154 °C (T_c), 323 °C (T_m)	—[b]	235 °C (T_m)	323 °C (T_m)	359 °C (T_m)	185 °C (T_g)	124 °C (T_g)
2nd heating	151 °C (T_g)	323 °C (T_m)	—[b]	81 °C (T_g), 148 °C (T_c), 235 °C (T_m)	190 °C (T_g)	169 °C (T_g)	191 °C (T_g)	119 °C (T_g)
T_g/T_m[c]	0.69	0.65	—	0.70	0.78	0.70	—	—
T_d in N_2	372 °C	461 °C	330 °C	398 °C	366 °C	445 °C	257 °C	326 °C

[a] Glassy state was obtained by quenching a liquid phase obtained on melting with liquid N_2. [b] No melting was observed before decomposition. [c] Ratio of absolute temperatures (K).

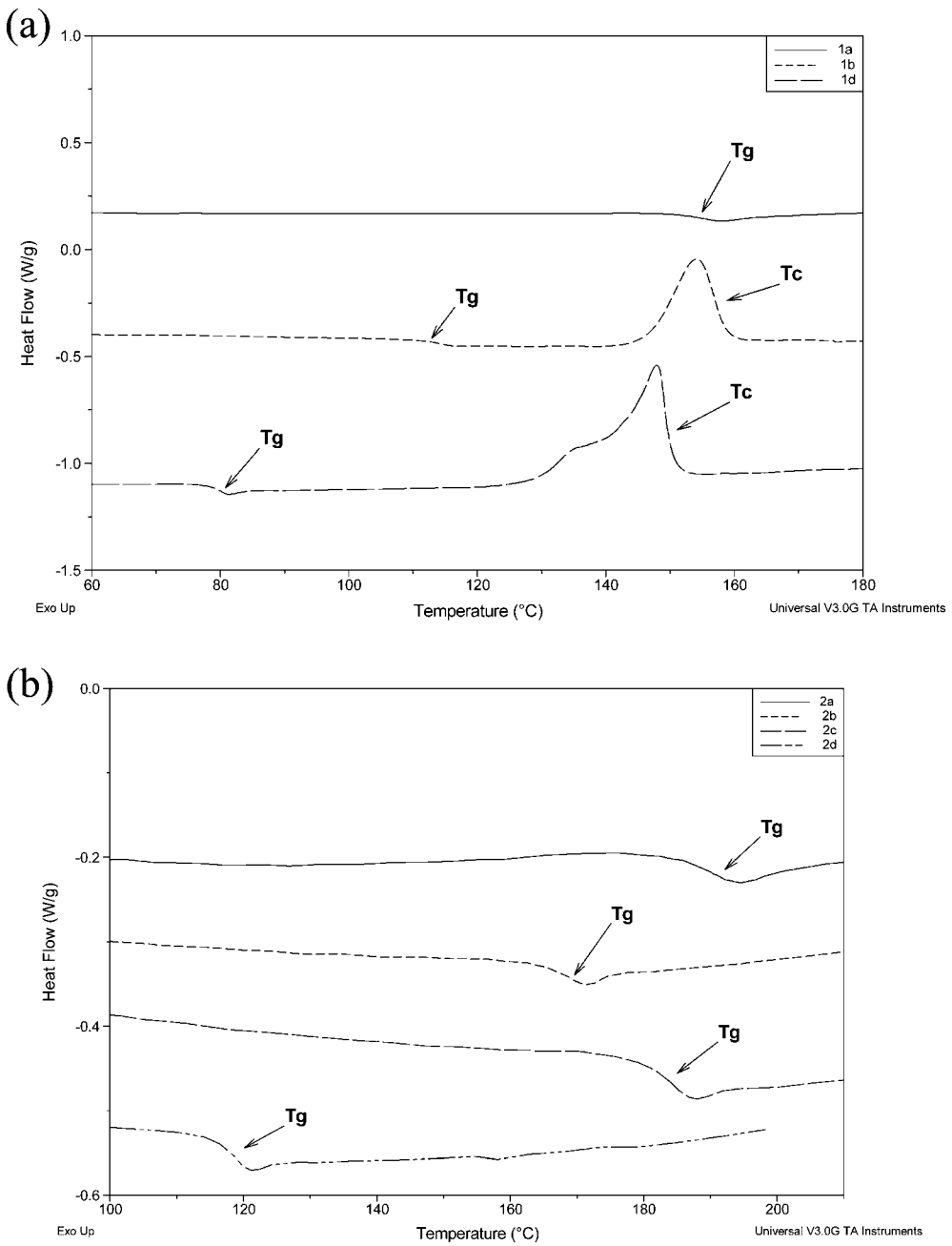

Fig. 1 DSC thermograms of (a) **1a** and **1d** obtained from the second heating cycle at heating and cooling rates of 10 °C min^{-1} in nitrogen and **1b** obtained from the first heating cycle of a liquid nitrogen-quenched sample at an identical heating rate; and (b) **2a–d** obtained from the second heating cycle at heating and cooling rates of 10 °C min^{-1} in nitrogen. Note that the usual crystal-to-liquid transition (T_m) values for **1b** and **1d** are not shown here for clarity, but they are included in Table 1.

(trifluoromethyl)phenyl]borate (X_4) resulted in the increase of 68 °C and 59 °C, respectively. X_4 had a reduced negative charge due to the electron-withdrawing trifluoromethyl groups compared to X_3, which explained the higher stability of **1d** and **2d** compared to **1c** and **2c**, respectively. The chemical modification of dications also had an important effect on the decomposition of these materials. The exchange of Y_1 to Y_2 generated a decrease of 6 °C, 16 °C, 73 °C and 72 °C for anions X_1, X_2, X_3, and X_4, respectively. These differences were presumably due to the electrophilic nature of the dication. Y_2, which had electron-withdrawing quinoline side groups, had weaker thermal stability compared to Y_1. These trends of the thermal stabilities should be noted when designing ionic amorphous molecular materials (Fig. S1b†).

X-Ray powder diffraction, polarizing optical, scanning electron microscopy and transmission electron microscopy

For further examination of the amorphous properties of the compounds, we used X-ray powder diffraction (XRD) studies.

The solvent induced crystals exhibited distinctive sharp peaks with high intensities denoting a high degree of crystallinity. In contrast, after melting these crystals followed by cooling, a glass was formed with broad peaks and low intensities in both small and wide angles; this is characteristic of an amorphous state. Representative XRD patterns of the crystal and the glass state of compound **2a** are given in Fig. S3†. When the compounds in this study were melted between two cover glasses uniform isotropic films were formed. Fig. 2a shows a representative polarized optical microscope (POM) photomicrograph of the glassy state of compound **2a** under a red quarter plate. Many cracks were seen in this film since it was cooled down quickly after melting. Alternatively, a steadier and slower cooling rate yielded a glassy film free from deformations. Interestingly enough, we were able to successfully draw fibers with a pair of tweezers from the melts of the compounds that formed the amorphous state. They were as long as six inches and their thickness was in the range of 50–120 μm. Fig. 2b shows an image of melt-drawn fiber of compound **2b** with a digital camera irradiated with UV light. To examine the morphology of these fibers, we examined them with POM and scanning electron microscopy (SEM) studies. The POM photomicrograph of the fiber of compound **2b** shown in Fig. 2c seemed to have a very smooth surface and no evidence of birefringence. This was also supported by the SEM image in Fig. 2d and 2e. In addition to the surface, we were able to examine the cross-section of these microfibers, which was also very uniform. This is the first example of ionic amorphous molecular material that is capable of forming these fibrous structures. Even though the mechanism of their formation and their orientations are not clear at this point, a combination of

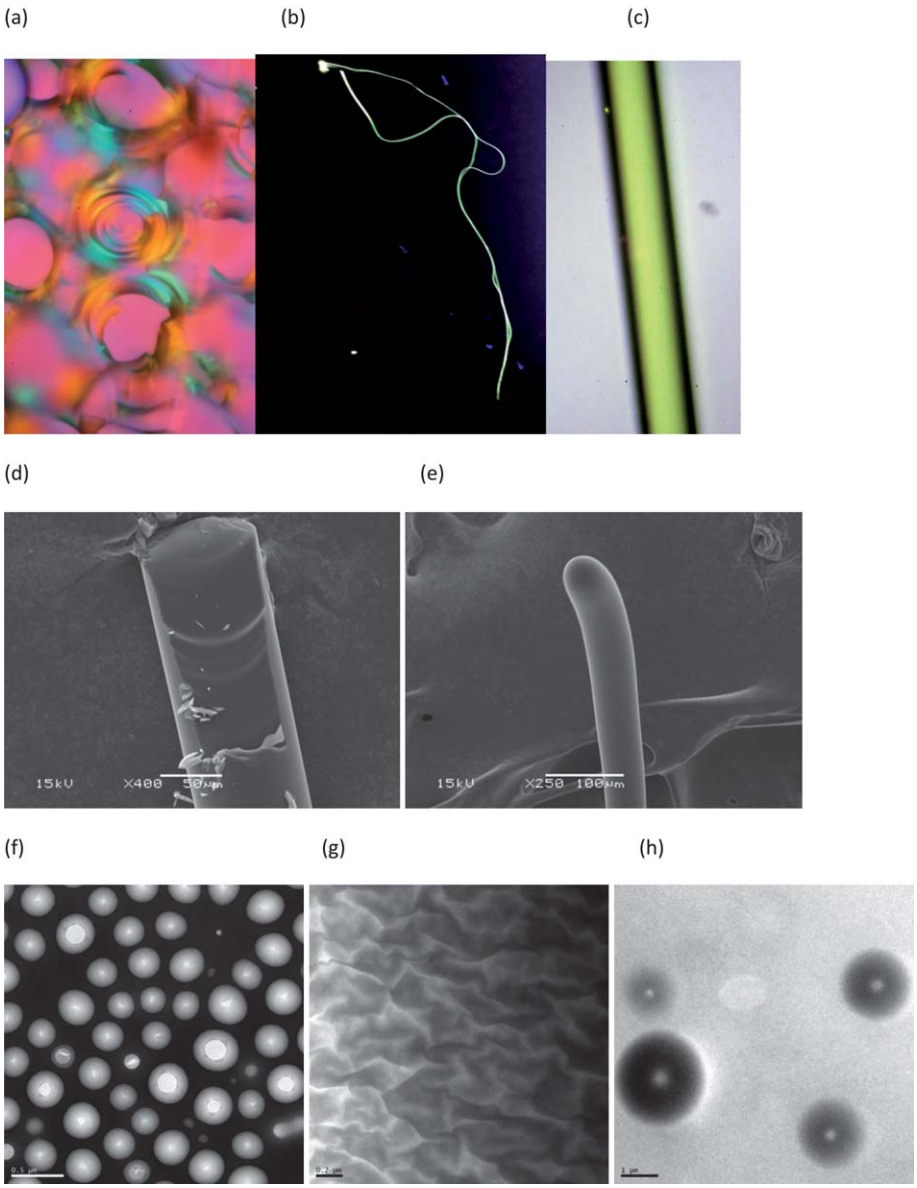

Fig. 2 (a) Photomicrograph of compound **2a** in deformed glassy state (magnification 400×), (b) photograph of hand-drawn fiber from the melt of compound **2b** irradiated with a hand-held UV light and (c) photomicrograph of the fiber from the melt of compound **2b** (400×); SEM images of the fibers from melts of (d) **2b** and (e) **2d**; and TEM images of (f) compound **2a** from 5 wt% CH_3OH solution (3900×) and compound **2b** (g) from 5 wt% THF solution (5000×) and (h) from 5 wt% CH_3CN solution (1700×).

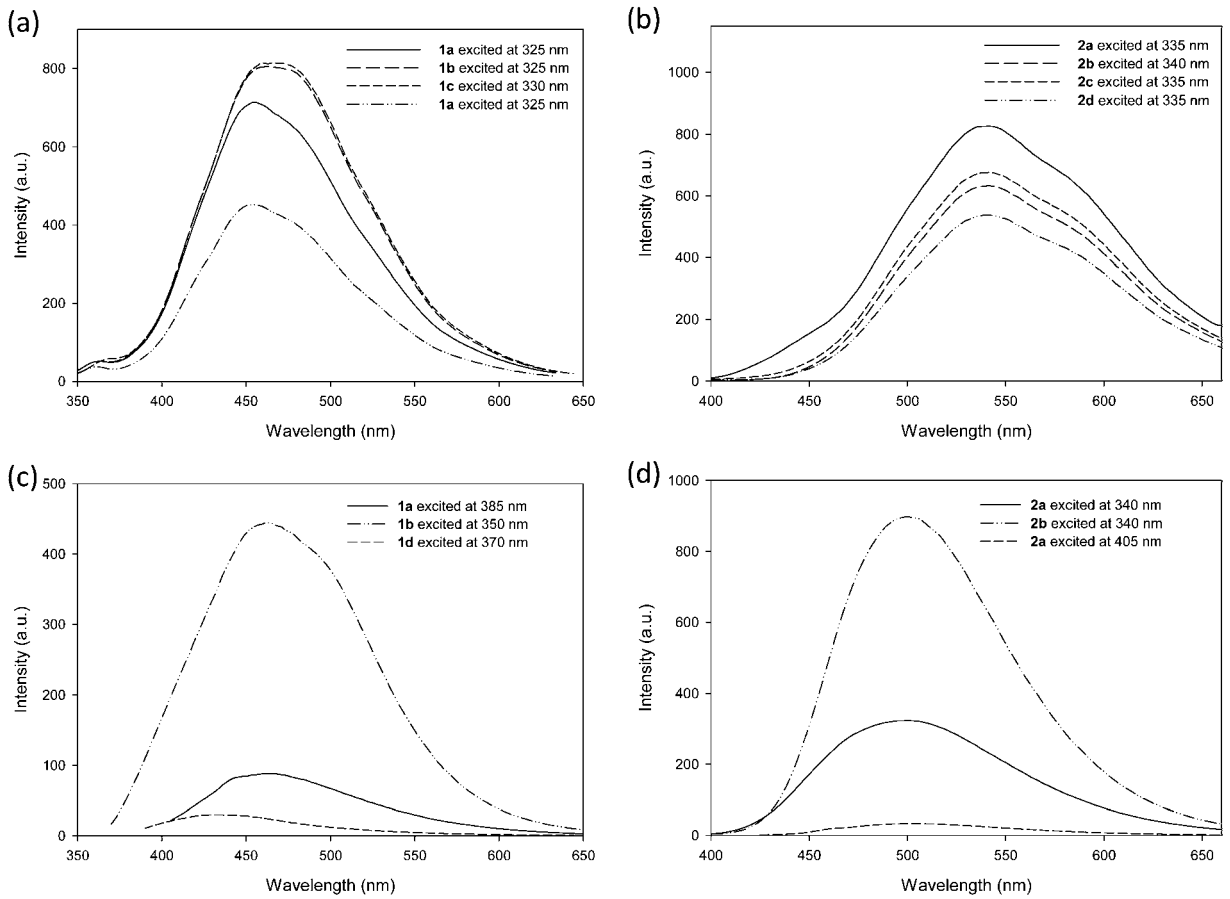

Fig. 3 Emission spectra of (a) compounds **1a–d** in acetonitrile, (b) compounds **2a** and**2b** in acetonitrile, (c) compounds **1a–d** cast from acetonitrile and (d) compounds **2a** and **2b** cast from acetonitrile at various excitation wavelengths.

intermolecular interactions including electrostatic, π–π stacking and van der Waals is a definite possibility. No birefringence was observed in POM studies; and these fibers exhibited only T_g values because of their amorphous nature. In the literature, most fibers generated through self-assemblies are pulled from organogels or by the phase transfer method. This is done by using a specific solvent or a combination of solvents that promote the formation of nanotubes, tapes or fibers.[23,24] TEM images from the solutions of these compounds in organic solvents revealed some interesting morphologies (Fig. 2f–h). In Fig. 2f, compound **2a** formed a film with numerous bubbles that were distributed uniformly throughout the film. Conversely, compound **2b** behaved differently in various organic solvents. In THF, it formed a thin film defined by extensive furrows and ridges (Fig. 2g). In a polar aprotic solvent such as acetonitrile, there was the development of doughnut-shaped microstructures throughout the sample (Fig. 2h).

Solubility in organic solvents

High solubility is a desired quality in both molecular and polymeric materials in order to efficiently process them into thin films and fibers. Generally, highly rigid materials such as Kevlar have limited solubility.[25] Even though the materials herein have relatively large molecular weights and are completely conjugated, their solubility in common organic solvents was exceptional. We were able to dissolve them into solvents with low polarity such as chloroform ($\varepsilon = 5.5$) and THF ($\varepsilon = 7.58$), solvents with medium polarity such as acetone ($\varepsilon = 23.1$) and solvents with high polarity such as methanol ($\varepsilon = 32.6$) acetonitrile ($\varepsilon = 37.5$) and DMSO ($\varepsilon = 47.2$). Their high solubility in various organic solvents is attributed to their inherent electrostatic charges as well as amorphous nature, which is in stark contrast with neutral conjugated molecular materials with poor solubility.[26,27]

UV-Vis and photoluminescent properties

Light emission is a unique property for many materials that can be utilized for many applications in modern science and technology. As such, it has recently become the focus for the development of optoelectronic devices.[5–12] Given the excellent solubility of these materials in various common organic solvents, we were able to study their fluorescence in different solvents with a wide range of polarities ($\varepsilon = 5.5$–37.5). The data of their optical properties including UV-Vis absorption, photoluminescence, and quantum yields are compiled in Table 2. The light emission spectra of the first set of compounds (**1a–d**) in CH_3CN are shown in Fig. 3a. They emitted blue light with λ_{em} values in the range of 454–467 nm when excited with 325–330 nm light. This small range denotes that the variation of the anions has a little effect on the light emission. Their full-width at half-maximum (fwhm) values were fairly high (100–110 nm), suggesting that the

Table 2 Optical properties of bis(pyridinium salt)s **1a–d** and **2a–d**

Compound	**1a**	**1b**	**1c**	**1d**	**2a**	**2b**	**2c**	**2d**
UV abs CH_3CN/nm	335	335	335	330	265, 340	265, 345	335	345
Band Gap/eV	3.31	3.31	3.31	3.31	3.26	3.26	3.26	3.26
PL λ_{em} $CHCl_3$/nm	401, 443	454	—[a]	424	511	532	489	529
PL λ_{em} THF/nm	463	395	—[a]	461	494	531	523	535
PL λ_{em} Acetone/nm	452	457	457	452	537	538	539	537
PL λ_{em} CH_3OH/nm	473	460	—[a]	476, 485	537	538	538	538
PL λ_{em} CH_3CN/nm	463	454	467	455	541	541	542	540
fwhm CH_3CN/nm	100	110	110	100	121	121	121	121
PL λ_{em} film/nm[b]	462	463	—[c]	432	500	500	—[c]	503
fwhm film/nm	105	120	—[c]	79	109	93	—[c]	90
Φ_F (%)[d]	1.1	1.0	0.9	1.3	2.1	1.8	1.2	1.5

[a] The compound was not soluble. [b] Thin film was cast from CH_3CN. [c] Light-emission from thin film was too weak to measure. [d] Quantum yield was calculated against diphenyl anthracene in cyclohexane as a standard ($\Phi_F = 0.9$).[28]

fluorescence behavior stemmed from multiple chromophores. The light emission properties of these ionic materials varied significantly with the change of polarity of organic solvents; these results were a manifestation of solvatochromic property. For example, compound **1a** emitted light with λ_{em} as low as 401 nm in $CHCl_3$ and λ_{em} as high as 473 nm in CH_3OH indicative of a bathochromic shift of 72 nm, suggesting that the excited state was more polar than the ground state. This result was the evidence of a positive solvatochromism property. Compounds **1b** and **1d** showed similar behavior with the differences of λ_{em} values of 68 nm and 61 nm, respectively. The poor solubility of compound **1c** in most organic solvents precluded to determine its light emission properties. Fig. 3b shows the photoluminescence spectra for the second set of compounds (**2a–d**). The modification of the dication from Y_1 to Y_2 resulted in a large bathochromic shift of 72–98 nm. This behavior was expected since the quinoline side groups further extended the conjugation of the dication, thus shifting the light emission bathochromically. The exchange of the anion had a negligible effect on the light emission in the solution state of materials **2a–d** as observed in the first set of compounds. Their fwhm values were quite large and increased compared with those of compounds **1a–d**. In the second set of materials, we also observed a positive solvatochromism. However, it was less pronounced than in the first set. The quantum yields of these ionic materials were studied in CH_3CN. They showed moderate values in the range of 0.9–2.1%; this is not very high for organic materials but is comparable to the values of polymeric materials. Their optical band gaps, determined from the onset of their UV-Vis absorption spectra, were in the range of 3.26 to 3.31 eV. These values are generally high for neutral light-emitting polymers[8,9] but are comparable to those of previously reported poly (pyridinium salt)s.[20,21]

Next, we explored the photoluminescent properties of these ionic materials in the thin films cast from CH_3CN to assess their potential for optoelectronic applications. The light emission spectra of the first set of materials are plotted in Fig. 3c. They exhibited λ_{em} values in the blue range similar to those in solutions. Their fwhm values were quite broad that ranged from 79–120 nm. In contrast, the λ_{em} values of compounds **2a–d** were shifted hypsochromically from solutions to solid states. They showed λ_{em} peaks in the narrow range of 500 nm to 503 nm, which is 38–42 nm less than those in CH_3CN solutions. These results suggested that they were less ordered in the solid state than in the solution state, which in turn, reducing the π–π stacking and causing a hypsochromic shift. Their fwhm values were also in the narrow range of 90–109 nm. Although we did not quantify their light emission efficiency in the solid state, but we observed that some anions affected the intensity of light emission significantly. For example, we were able to make films of **1c** and **2c**, which had an X_3 anion, but their light emissions were too low to measure. Interestingly, compounds **1d** and **2d**, which had an X_4 anion, did have detectable light emission, even though their intensities were low (Fig. 3c and d). The light emission properties of **1d** and **2d** can be attributed to the presence of trifluoromethyl electron-withdrawing groups in the aromatic moieties.

The light-emission properties of amorphous ionic molecular materials are mainly affected by chemical structural modifications of the dications, because the primary chromophore is located in the chemical structures of dications. Generally, anions in this study seemed to have little effect on the light emission in solution. In contrast, they played an important role in the light emission and quantum yields in the solid state as observed in the cases of **1c**, **1d**, **2c**, and **2d**. The extensive optical studies performed on this novel class of amorphous ionic molecular materials could serve as an essential guideline of how their optical properties could be fine-tuned for their potential applications. We also briefly examined their potential as fluorophores in the biological systems. As examined with fluorescence microscopy studies (Fig. S7 and 8†), an aliquot of 100 μg mL^{-1} solution of compound **2a** in phosphate-buffered saline (PBS) successfully stained cancer cells within 20 min and, therefore, they could be potentially used as fluorophores for staining various cellular materials. Additionally, DNA electrophoresis gels stained with compound **1a** showed binding with the DNA, but the fluorescence output was weaker compared with that of ethidium bromide, which may be an indication of the extent of their binding abilities *via* electrostatic interactions (Fig. S9†). These preliminary data show that some of these ionic compounds have some activity towards biological molecules, the potential of which remains to be explored.

Conclusions

We prepared a series of new photoactive amorphous ionic materials *via* both ring-transmutation and metathesis reactions. They displayed very good thermal stabilities that were dependent

on the nature of both the anions and the dications. Most of these compounds vitrified successfully upon slow cooling after melting the solvent-induced crystals. They had excellent solubilities in a wide range of common organic solvents. They can be processed easily into thin films and fibers from their melts or solutions, thereby avoiding cumbersome and expensive techniques such as vapor deposition technique.[3] Additionally, their luminescence properties produced blue and green light in both the solution and solid states. Their quantum yields were moderate. Here, we demonstrated a versatile method for the synthesis of a novel class of materials and how their physical properties could be fine-tuned. These amorphous ionic materials combine into one the excellent properties of both conventional amorphous materials and ionic compounds. They are homogeneous, transparent and easy to process. These new smart materials could be used as components for OLEDs, LECs, OFEDs, organic laser, and even as solid electrolytes for battery applications. They constitute a class of materials at the frontier of ionic liquids, conventional molecular glasses and ionic polymers and display unique properties unattainable with other related class of materials.

Experimental section

Starting materials and synthesis of intermediates

4,4′(1,4-Phenylene)bis(2,6-diphenylpyrylium)ditosylate[19] and sodium tetrakis[3,5-bis(trifluoromethyl)phenyl]borate[29] were prepared according to the known procedures. The synthesis of the 2,4-diphenylquinolin-6-amine will be reported elsewhere. The other starting compounds and reagents were purchased from either Sigma-Aldrich or TCI and were used as received.

Compound 1a. 5.00 g (5.66 mmol) 4,4′(1,4-phenylene)bis(2,6-diphenylpyrylium)ditosylate and 1.11 g (11.9 mmol) aniline were added in 50 mL of DMSO. The reaction was kept at 130–140 °C for 24 h under nitrogen. After completion of the reaction, the reaction flask was cooled down to room temperature and the product was precipitated out in water. The precipitate was washed with acetone and air-dried It was then recrystallized from ethanol/methanol mixture to yield 5.00 g (4.41 mmol, yield 79%) of off-white fluffy crystals. ^{1}H NMR (400 MHz, d_6-DMSO) δ ppm 8.84 (s, 4H), 8.65 (s, 4H), 7.53–7.43 (m, 16H), 7.42–7.31 (m, 12H), 7.19 (m, 6H), 7.08 (d, J = 7.88 Hz, 4H), 2.26 (s, 6H); ^{13}C NMR (100 MHz, d_6-DMSO) δ ppm 156.4, 153.8, 145.7, 138.9, 137.4, 136.6, 132.9, 129.9, 129.8, 129.8, 129.6, 128.5, 128.4, 128.0, 127.9, 125.5, 125.4, 20.7; Anal. calcd for $C_{66}H_{52}N_2S_2O_6$: C 76.72, H 5.07, N 2.71, S 6.21; found: C 76.50, H 5.00, N 2.74, S 6.15%.

Compound 2a. The identical reaction procedure was followed as for the preparation of compound **1a** but 2,4-diphenylquinolin-6-amine was used instead of aniline as starting material. The crude product was recrystallized from ethanol/methanol mixture to yield 3.60 g (2.50 mmol, yield 89%) of beige crystals. ^{1}H NMR (400 MHz, d_6-DMSO) δ ppm 8.85 (s, 4H), 8.66 (s, 4H), 8.33–8.24 (m, 4H), 8.05 (d, J = 1.76 Hz, 4H), 7.95 (d, J = 8.99 Hz, 2H), 7.85 (dd, J = 9.02, 2.29 Hz, 2H), 7.68–7.58 (m, 6H), 7.58–7.51 (m, 6H), 7.51–7.45 (m, 12H), 7.45–7.37 (m, 12H), 7.16–7.06 (m, 8H), 2.27 (s, 6H); ^{13}C NMR (100 MHz, d_6-DMSO) δ ppm 157.6, 156.4, 153.9, 149.0, 147.1, 145.8, 137.7, 137.3, 136.8, 136.6, 136.2, 133.1, 130.1, 130.0, 129.9, 129.8, 129.7, 129.5, 128.9, 128.8, 128.7, 128.2, 127.9, 127.5, 126.9, 125.6, 125.4, 123.5, 119.9, 20.7; Anal. calcd for $C_{96}H_{70}N_4S_2O_6$: C 80.09, H 4.90, N 3.89, S 4.45; found: C 79.89, H 4.91, N 3.87, S 4.43%.

Compound 1b. 1.00 g (0.886 mmol) compound **1a** was dissolved in 25 mL of methanol. 0.534 g (1.86 mmol) lithium triflimide was dissolved in a minimum amount of methanol. They were added together and a white precipitate formed quickly. The reaction was kept at 40 °C overnight to ensure completion. The product was precipitated out and washed with water. It was recrystallized from methanol to yield 1.06 g (0.847 mmol, yield 96%) of white crystals. ^{1}H-NMR (400 MHz, d_6-DMSO) δ ppm 8.87 (s, 4H), 8.66 (s, 4H), 7.50–7.43 (m, 15H), 7.39 (m, 15H); ^{13}C-NMR (100 MHz, d_6-DMSO) δ ppm 156.4, 153.0, 138.9, 136.6, 132.9, 129.9, 129.7, 129.6, 128.5, 128.0, 125.5, 121.0, 117.8; Anal. Calcd for $C_{56}H_{38}N_4S_4O_8F_{12}$: C 53.76, H 3.06, N 4.48, S 10.25; found: C 54.01, H 2.95, N 4.58, S 10.33%.

Compound 2b. The similar reaction procedure was followed as for the preparation of compound **1b** by using a compound **2a** instead of compound **1a**. The crude product was recrystallized from methanol to yield 0.530 g (0.320 mmol, yield 92%) of yellow crystals. ^{1}H NMR (400 MHz, d_6-DMSO) δ ppm 8.87 (s, 4H), 8.67 (s, 4H), 8.29 (dd, J = 7.49, 2.14 Hz, 4H), 8.05 (d, J = 2.48 Hz, 4H), 7.96 (d, J = 8.98 Hz, 2H), 7.83 (dd, J = 9.03, 2.27 Hz, 2H), 7.70–7.58 (m, 6H), 7.58–7.51 (m, 6H), 7.45 (m, 20H), 7.12 (dd, J = 7.79, 1.47 Hz, 4H); ^{13}C NMR (100 MHz, d_6-DMSO) δ ppm 157.6, 156.5, 153.9, 149.0, 147.1, 137.7, 136.8, 136.7, 136.2, 133.1, 130.1, 130.1, 130.0, 129.8, 129.7, 129.5, 129.4, 128.8, 128.2, 127.5, 126.9, 125.6, 123.6, 121.0, 119.9, 117.8; Anal. calcd for $C_{86}H_{56}N_6S_4O_8F_{12}$: C 62.31, H 3.41, N 5.07, S 7.72; found: C 62.28, H 3.18, N 5.12, S 7.76%.

Compound 1c. 0.500 g (0.441 mmol) compound **1a** was dissolved in 25 mL of methanol. 0.318 g (0.928 mmol) sodium tetraphenylborate was dissolved in minimum amount of water. They were added together and a yellow precipitate formed quickly. The reaction was kept at 40 °C overnight to ensure completion. The precipitate was collected and washed with water. It was then recrystallized from acetonitrile to yield 0.450 g (0.345 mmol, yield 79%) of yellow crystals. ^{1}H NMR (400 MHz, d_6-DMSO) δ ppm 8.84 (s, 4H), 8.64 (s, 4H), 7.50–7.41 (m, 12H), 7.41–7.33 (m, 12H), 7.23–7.13 (m, 22H), 6.91 (t, J = 7.4 Hz, 16H), 6.78 (t, J = 7.2 Hz, 8H); ^{13}C NMR (100 MHz, d_6-DMSO) δ ppm 164.5, 164.0, 163.5, 156.9, 154.3, 139.4, 137.1, 135.9, 133.4, 130.4, 130.4, 130.2, 128.9, 128.5, 126.0, 125.7, 121.9; Anal. calcd for $C_{98}H_{78}N_2B_2$: C 90.17, H 6.02, N 2.15; found: C 90.15, H 5.85, N 2.22%.

Compound 2c. The similar reaction procedure was followed as for the preparation of compound **1c** but compound **2a** was used instead of compound **1a**. The crude product was eluted in chloroform through a column chromatography over silica gel. The volume of chloroform was reduced under reduced pressure and the pure compound was precipitated out in hexane to yield 0.400 g (0.230 mmol, yield 66%) of light brown solid. ^{1}H NMR (400 MHz, d_6-DMSO, 50 °C) δ ppm 8.81 (s, 4H), 8.60 (s, 4H),

8.31–8.22 (m, 4H), 8.05–7.96 (m, 4H), 7.94 (d, $J = 8.98$ Hz, 2H), 7.80 (dd, $J = 8.95$, 2.23 Hz, 2H), 7.68–7.56 (m, 6H), 7.56–7.49 (m, 6H), 7.49–7.42 (m, 8H), 7.42–7.30 (m, 12H), 7.25–7.15 (m, 16H), 7.15–7.06 (m, 4H), 6.90 (t, $J = 7.40$ Hz, 16H), 6.77 (t, $J = 7.17$ Hz, 8H); ^{13}C NMR (100 MHz, d_6-DMSO) δ ppm 164.1, 163.6, 163.1, 162.6, 157.7, 156.6, 154.1, 149.1, 147.2, 137.8, 136.7, 136.7, 136.3, 135.5, 133.0, 130.1, 130.0, 129.9, 129.7, 129.4, 128.8, 128.7, 128.2, 127.5, 126.9, 125.7, 125.1, 123.7, 121.4, 119.9; Anal. calcd for $C_{130}H_{96}N_4B_2$: C 89.95, H 5.57, N 3.23; found: C 90.10, H 5.51, N 3.27%.

Compound 1d. 0.300 g (0.265 mmol) compound **1a** was dissolved in 25 mL of methanol. 0.490 g (0.556 mmol) sodium tetrakis[3,5-bis(trifluoromethyl)phenyl]borate was also dissolved in a minimum amount of methanol. They were added together. The reaction was kept at 40 °C overnight to ensure completion. The desired product was precipitated out and washed with copious amount of water. It was further purified by recrystallized from isopropanol/water to yield 0.500 g (0.207 mmol, yield 78%) of off-white crystals. ^{1}H NMR (400 MHz, d_6-DMSO) δ ppm 8.89 (s, 4H), 8.70 (s, 4H), 7.71 (s, 8H), 7.68–7.60 (m, 16H), 7.49 (m, 12H), 7.44–7.35 (m, 12H), 7.22 (dd, $J = 6.32$, 2.88 Hz, 6H); ^{13}C NMR (100 MHz, d_6-DMSO) δ ppm 161.7, 161.2, 160.7, 160.2, 156.5, 153.9, 139.0, 136.7, 134.1, 134.0, 133.0, 129.7, 128.6, 128.1, 125.6, 122.6, 119.9, 117.7; Anal. calcd for $C_{116}H_{62}N_2B_2F_{48}$: C 57.64, H 2.59, N 1.16; found: C 57.54, H 2.43, N 1.18%.

Compound 2d. The identical reaction procedure was followed as for the preparation of compound **1d** but compound **2a** was used instead of compound **1a**. The crude product was eluted in chloroform through column chromatography over silica gel. The impurities eluted out first of the column and the main product was then eluted out with the addition of methanol. The solvent methanol was removed under reduced pressure to give an oily viscous liquid. It was then dissolved in chloroform and precipitated out slowly with the addition of hexane to yield 0.410 g (0.145 mmol, yield 70%) of yellow solid. ^{1}H NMR (400 MHz, d_6-DMSO) δ ppm 8.89 (s, 4H), 8.70 (s, 4H), 8.31 (dd, $J = 7.43$, 1.94 Hz, 4H), 8.07 (d, $J = 3.01$ Hz, 4H), 7.98 (d, $J = 9.00$ Hz, 2H), 7.86 (dd, $J = 8.97$, 2.16 Hz, 2H), 7.72 (s, 9H), 7.67–7.62 (m, 22H), 7.57 (m, 6H), 7.53–7.48 (m, 8H), 7.47–7.39 (m, 12H), 7.14 (d, $J = 6.54$ Hz, 4H); ^{13}C NMR (100 MHz, d_6-DMSO) δ ppm 161.7, 161.2, 160.7, 160.2, 157.7, 156.6, 154.0, 149.1, 147.2, 137.8, 136.9, 136.8, 136.3, 134.1, 134.0, 133.2, 130.2, 130.0, 129.8, 129.6, 129.5, 128.8, 128.7, 128.3, 127.6, 127.0, 125.7, 125.4, 123.7, 122.6, 120.0, 117.7; Anal. calcd for $C_{146}H_{80}N_4B_2F_{48}$: C 62.10, H 2.86, N 1.98; found: C 61.83, H 2.68, N 1.95%.

Acknowledgements

P.K.B. acknowledges the University of Nevada Las Vegas for an Applied Research Initiative, the donors of the Petroleum Research Fund, administered by the American Chemical Society, and an award (CCSA# CC5589) from Research Corporation for the support of this research. A.K.N. acknowledges the Graduate College (UNLV) for providing him a Nevada Stars Graduate Assistantship for the period of 2006–2008. The work is in part supported by the NSF under Grant No. 0447416 (NSF EPSCoR RING-TRUE III), NSF-Small Business Innovation Research (SBIR) Award (Grant OII-0610753), NSF-STTR Phase I Grant No. IIP-0740289, and NASA GRC Contract No. NNX10CD25P. We also sincerely acknowledge Dr Longzhou Ma for his expertise in the analyses of TEM studies and Van Vo for her expertise in fluorescence microscopy studies.

References

1 P. G. Debenedetti and F. H. Stillinger, *Nature*, 2001, **410**, 259.
2 F. H. Stillinger, *Science*, 1995, **267**, 1935.
3 S. F. Swallen, K. L. Kearns, M. K. Mapes, Y. S. Kim, R. J. McMahon, M. D. Ediger, T. Wu, L. Yu and S. Satija, *Science*, 2007, **315**, 353.
4 Y. Shirota, *J. Mater. Chem.*, 2000, **10**, 1.
5 Y. Shirota, *J. Mater. Chem.*, 2005, **15**, 75.
6 Y. Shirota and H. Kageyama, *Chem. Rev.*, 2007, **107**, 953.
7 P. Strohriegl and J. V. Grazulevicius, *Adv. Mater.*, 2002, **14**, 1439.
8 R. H. Friend, R. W. Gymer, A. B. Holmes, J. H. Burroughes, R. N. Marks, C. Taliani, D. D. C. Bradley, D. A. D. Santos, J. L. Bredas, M. Logdlund and W. R. Salaneck, *Nature*, 1999, **397**, 121.
9 U. Mitschke and P. Bauerle, *J. Mater. Chem.*, 2000, **10**, 1471.
10 A. P. Kulkarni, C. J. Tonzola, A. Babel and S. A. Jenekhe, *Chem. Mater.*, 2004, **16**, 4556.
11 Q. Pei, G. Yu, C. Zhang, Y. Yang and A. J. Heeger, *Science*, 1995, **269**, 1086.
12 N. Tessler, *Adv. Mater.*, 1999, **11**, 363.
13 J. S. Wilkes, *Green Chem.*, 2002, **4**, 73.
14 C. Baudequin, D. Brégeon, J. Levillain, F. Guillen, J.-C. Plaquevent and A.-C. Gaumont, *Tetrahedron: Asymmetry*, 2005, **16**, 3921.
15 T. L. Greaves and C. J. Drummond, *Chem. Rev.*, 2007, **108**, 206.
16 P. Kubisa, *Prog. Polym. Sci.*, 2004, **29**, 3.
17 M. J. Earle, J. M. S. S. Esperanca, M. A. Gilea, J. N. Canongia Lopes, L. P. N. Rebelo, J. W. Magee, K. R. Seddon and J. A. Widegren, *Nature*, 2006, **439**, 831.
18 W. L. Hough-Troutman, M. Smiglak, S. Griffin, W. M. Reichert, I. Mirska, J. Jodynis-Liebert, T. Adamska, J. Nawrot, M. Stasiewicz, R. D. Rogers and J. Pernak, *New J. Chem.*, 2009, **33**, 26.
19 D. R. MacFarlane and M. Forsyth, *Adv. Mater.*, 2001, **13**, 957.
20 P. K. Bhowmik, R. A. Burchett, H. Han and J. J. Cebe, *J. Polym. Sci., Part A: Polym. Chem.*, 2001, **39**, 2710.
21 P. K. Bhowmik, H. Han and A. K. Nedeltchev, *Polymer*, 2006, **47**, 8281.
22 H. Han, P. R. Vantine, A. K. Nedeltchev and P. K. Bhowmik, *J. Polym. Sci., Part A: Polym. Chem.*, 2006, **44**, 1541.
23 J. P. Hill, W. Jin, A. Kosaka, T. Fukushima, H. Ichihara, T. Shimomura, K. Ito, T. Hashizume, N. Ishii and T. Aida, *Science*, 2004, **304**, 1481.
24 D. S. Tsekova, B. Escuder and J. F. Miravet, *Cryst. Growth Des.*, 2007, **8**, 11.
25 J. Lin and D. Sherrington, *Adv. Polym. Sci.*, 1994, **111**, 177.
26 C. J. Tonzola, A. P. Kulkarni, A. P. Gifford, W. Kaminsky and S. A. Jenekhe, *Adv. Funct. Mater.*, 2007, **17**, 863.
27 J. M. Hancock, A. P. Gifford, Y. Zhu, Y. Lou and S. A. Jenekhe, *Chem. Mater.*, 2006, **18**, 4924.
28 J. N. Demas and G. A. Crosby, *J. Phys. Chem.*, 1970, **75**, 991.
29 H. Iwamoto, T. Sonoda and H. Kobayashi, *Tetrahedron Lett.*, 1983, **24**, 4703.

